IEEE Access
Multidisciplinary ⋮ Rapid Review ⋮ Open Access Journal

Received 19 February 2024, accepted 26 February 2024, date of publication 4 March 2024, date of current version 8 March 2024.

Digital Object Identifier 10.1109/ACCESS.2024.3373309

RESEARCH ARTICLE

Malicious UAV Detection Over Rician Fading Channel: Performance Analysis

YOUSEF AWAD, (Student Member, IEEE), AND SUHAIL AL-DHARRAB, (Senior Member, IEEE)

Electrical Engineering Department, King Fahd University of Petroleum and Minerals (KFUPM), Dhahran 31261, Saudi Arabia
Center for Communication Systems and Sensing, King Fahd University of Petroleum and Minerals (KFUPM), Dhahran 31261, Saudi Arabia

Corresponding author: Suhail Al-Dharrab (suhaild@kfupm.edu.sa)

This work was supported by the Deanship of Research Oversight and Coordination (DROC), King Fahd University of Petroleum and Minerals (KFUPM), through the Interdisciplinary Research Center for Communication Systems and Sensing, under Project INCS2113.

ABSTRACT Unmanned aerial vehicles (UAVs) are predicted to be widely used in both military and civilian sectors in the coming years due to their high mobility, low cost, and enhancement of the line-of-sight (LoS) conditions in non-terrestrial networks. Nevertheless, this raises some security concerns if they are manipulated to cause security threats in restricted locations, or even cause privacy breaches. In order to detect malicious UAVs, radio frequency (RF)-based approaches are adopted to detect ambient RF signals, which can be accomplished with inexpensive RF sensors under both LoS and, in particular, non-line-of-sight (NLoS) conditions. In this paper, we propose a passive detection technique based on received signal strength (RSS), and derive analytical expressions on the detection and false alarm probabilities considering realistic air-to-ground (A2G) channel conditions. A novel low-complexity suboptimal detector is also proposed and its performance is compared to the optimal detection. Monte Carlo simulations are used to confirm the accuracy of the derived expressions under the aforementioned channel conditions. Our mathematical framework, analytical derivations, and simulation results reveal that the sensing node can achieve an accuracy of 0.9 under LoS scenarios, where the NLoS conditions cause some challenges in the accuracy of detection. The proposed low-complexity suboptimal detector for urban and suburban environments has close performance compared to the optimal detection.

INDEX TERMS Air-to-ground (A2G), log-likelihood ratio, receiver operating characteristic (ROC), sufficient statistic.

I. INTRODUCTION

Unmanned aerial vehicles (UAVs) have been widely utilized in several applications and can provide multiple services in environmental protection, traffic events and congestion monitoring [1], agriculture and public safety [2]. However, as the use of UAVs is rapidly increasing, the potential threats are increasing as well, especially if they have been controlled to breach into highly restricted areas as in oil and gas facilities or possible privacy invasions of others. Threats of UAVs may include physical threats such as explosives, radioactive materials and guns or cyber threats such as hijacking, spoofing, and hacking [3]. There are several examples in which the presence of UAVs can be a real threat. One example of the harmful impact of UAVs is their unauthorized presence in critical areas, such as airports or restricted airspace. This poses significant safety risks, including potential collisions with manned aircraft, interference with air traffic control systems, and disruption of airport operations. Detecting and mitigating these unauthorized UAVs are of utmost importance to ensure the safety and security of aviation operations. These man-made flying objects, often known as drones, are difficult to identify and track in real-time in urban areas because they typically have a low altitude, moderate speed, and small radar cross-section (RCS) [4], [5], [6]. Counter unmanned aerial systems in the market depend on radar [7], computer vision [8], [9], radio frequency (RF) [10], [11], and acoustic sensors [12]. These systems struggle to identify

The associate editor coordinating the review of this manuscript and approving it for publication was Cong Pu.

© 2024 The Authors. This work is licensed under a Creative Commons Attribution-NonCommercial-NoDerivatives 4.0 License.
For more information, see https://creativecommons.org/licenses/by-nc-nd/4.0/

TABLE 1. Comparison of UAV detection systems.

Method	Advantages	Disadvantages
Ambient RF	works in NLoS, passive, weather independent	autonomous UAV flights, jamming scenarios
Radar	detect autonomous UAVs, micro-Doppler signature accurate in LoS conditions	power consumption, small RCS of drone, high cost and complexity
Computer Vision	fits all UAV types, passive, accuracy (optical sensors)	requires LoS, affected by weather, high cost
Acoustic	low cost (microphones), works in NLoS	acoustic background noise and weather

such intruding UAVs and are susceptible to being tricked, leading to false alarms or false negatives, i.e. missed targets. These approaches have advantages and disadvantages of their own, and occasionally they are combined to improve the precision of detection and tracking of the intruding UAV. For example, one of the main advantages of using RF-based detection techniques is the fact that it is passive. In other words, the sensing node only receives (or senses) the signal emitted from the intruding UAV. The use of radar, on the other hand, will consume more energy compared to our proposed approach. However, in the case of autonomous or jammer-aided UAVs [13], the RF-based detection systems will not detect them while radar-based or similar techniques, such as those based on computer vision, become essential. Multiple receiving antenna elements at the RF sensor can enhance the direction of arrival estimation of the sensed RF signal. Some of the existing solutions for counter unmanned aerial systems rely on RF direction finding (RFDF) sensors which effectively detect the signal of interest in congested spectrum environments. A summary of the advantages and disadvantages of each approach is presented in Table 1. The aim of this work is to suggest a low-cost passive method for identifying malicious UAVs in a variety of channel and environment states.

A. RELATED WORKS

1) RF-BASED UAV DETECTION

Ambient RF signals emitted from the malicious UAV can be sensed at the terrestrial RF network under mixed channel propagation conditions. In [5], Sinha et al. investigated the fundamental limits on the drone detection probability under mixed line-of-sight (LoS) and non-line-of-sight (NLoS) conditions using directional three-dimensional (3D) antenna patterns. They evaluated the detection probability numerically, which requires averaging over all possible locations of interfering sources and base stations using the Stable probability distribution. Soltani et al. in [10] proposed RF fingerprinting with multi-classifier scheme using two-step score-based aggregation method to enhance the overall accuracy of UAV detection and classification. Massive IoT network with multiple RF-based sensors was considered in [11] assuming Rayleigh fading channel, and the detection performance was investigated using Neyman-Pearson criterion. However, in [11], the work focused on multipath fading under the NLoS conditions but not the LoS condition, where it is crucial and most likely to occur in the presence UAV detected by a ground sensing node. In [14], Nie et al. presented detection and identification schemes based on Wi-Fi signal and RF fingerprint under both indoor and outdoor scenarios.

Furthermore, learning-based algorithms have been merged with RF-based detection more often recently. For instance, the problem of detection and classification of UAVs in the presence of wireless interference signals was investigated by Ezuma et al. in [15] specifically for Wi-Fi and Bluetooth emitters using proper machine learning technique. In [16], the authors proposed a software defined radio (SDR) platform called DronEnd, which has the ability to scan the spectrum of RF signals for detecting the presence of the drone. Its location is identified via angle-of-arrival (AoA) estimation algorithms and disrupting the communication between the operator/controller and the drone through jamming signals. In [17], the k-nearest neighbor (k-NN) machine learning classification method merged with RF Fingerprints were utilized for micro-UAV detection and classification with an average accuracy of 0.96. In [18], multiple deep learning algorithms have been used for detection and classification of drones based on RF compressed signals. Experimental results in [19] showed that the proposed hierarchical learning approach has outperformed other techniques with an accuracy rate of 0.99. Convolutional neural network (CNN) had been utilized in [20] to develop a noise immune UAV signal classification system which had been tested at different signal-to-noise ratios (SNRs). Support vector machine (SVM), artificial neural network (ANN), decision tree (DT), and random forest (RandF) classifiers had been utilized in [21] for detection and classification of drones in the presence of Wi-Fi interference using UAV video signal (VS) fingerprints where indoor and outdoor experiments were carried out with high accuracy rates, especially by using RandF.

Hu et al. derived the optimal decision rule using the log-likelihood ratio (LLR) in [22] where multiple antennas were utilized with beam sweeping at the sensing node. Moreover, in [23], a data integrity technique called MaDe was utilized to identify malicious UAVs using a generalized likelihood ratio test. The performance analysis demonstrated that MaDe identified malicious UAVs with high accuracy and limited time delay.

2) OTHER DETECTION TECHNIQUES

Due to their robustness and versatility, radar-based sensors are nowadays important for UAV detection and classification [4], [24], [25], [26]. In [7], a UAV classification model has been proposed using Deep Convolutional Neural Network (DCNN) where the training data set contains a Range-Doppler (RD) map of a frequency-modulated continuous-wave (FMCW) radar of a moving UAV. Generative Adversarial Network was further used for data augmentation, where an accuracy rate of 0.909 was achieved in large

TABLE 2. Related works on UAV detection.

	This Paper	[5]	[11]	[23]	[22]	[14]	[15]	[10]
Analysis Type	Analytical/ Simulation	Stochastic geometry/ Simulation	Analytical/ Simulation	Data analysis	Analytical/ Simulation	Experimental/ ML	Experimental/ ML	Experimental/ ML
Decision Criteria	LLR	N/A	Neyman-Pearson	LLR	LLR	Fixed threshold	Fixed threshold	Probability and ratio thresholds
Fading Channel Model	Rician (realistic)	Rician (realistic)	Rayleigh	N/A	Rayleigh	N/A	N/A	N/A
Interference Analysis	N/A	Cellular mobile users	N/A	N/A	N/A	N/A	Wi-Fi and Bluetooth	N/A
Complexity (cost)	Low	Moderate	Low	Low	Moderate	High	High	High

data scenarios. Authors in [27] provide experimental and analytical investigation of micro UAV detection in a rocky terrain using a low grazing angle, surface-sited 24 GHz dual polarized FMCW radar. The problem of defining the type of the detected UAV was considered as an M-ary hypothesis testing problem by Ezuma et al. in [28]. In target classification, the authors used maximum a posteriori probability (MAP) decision rule, which is optimal for a given set of RCS data. Such RCS-based UAV statistical recognition system determines its class membership. Multiple-input multiple-output (MIMO) radar can also be used to detect intruding UAVs where the multiple phased arrays with spaced digital receivers and waveform generators are across radar aperture [29].

Recently, the aid of computer vision in target detection and tracking has developed rapidly due to its ability to provide high performance systems [30], [31], [32]. In [9], a Dalian University of Technology (DUT) Anti-UAV dataset was used on several existing detection algorithms for performance evaluation and comparison with a proposed detection and tracking algorithm that showed high performance by experiments. Opromolla et al. in [33] proposed a template matching and morphological filtering-based detection and tracking algorithms on cooperative applications. The algorithm's performance was assessed by a flight test campaign where the accuracy of target position was in the order of one pixel and the percentage of correct detection decisions was in the range of 0.85-0.95.

On the other hand, acoustic-based algorithms has proven to be promising and feasible for short range drones surveillance [34], [35], [36]. In [12], SVM-based method has been used for UAV sounds classification among birds, airplanes or thunderstorms. An accuracy of 0.97 was achieved using Mel-frequency cepstral coefficients (MFCC) features extraction technique. In [37], a 24/7 detection and localization scheme was proposed using time difference of arrival (TDoA) estimation algorithm, which is based on the Bayesian filter. Experimental results showed that the proposed model can achieve high detection and localization accuracy. Finally, a real-time detection was proposed by Liu et al. in [38] using pruned-YOLOv4 model and compared to RetinaNet, fully convolutional one-stage object detector (FCOS), YOLOv3, and YOLOv4. Experiment results showed that their proposed model achieved higher accuracy with less processing time.

B. CONTRIBUTIONS

The main contributions of our work in this paper are summarized as follows.

- Detection performance is investigated and closed-form expressions are derived for a low-cost passive RF detector taking into consideration realistic Rician fading channel model.
- A low-complexity suboptimal detector for the UAV in urban and suburban environments is proposed, and its performance is compared with the optimal one.

For easier comparison, Table 2 presents the related works and the state-of-the-art papers in our literature review (N/A stands for not applicable).

The rest of the paper is organized as follows. In Section II, our system model is presented. Section III introduces the UAV detection problem, while detection performance derivations and the performance of the proposed optimal and suboptimal detectors are analyzed in Section IV. The numerical results are presented and discussed in Section V. Finally, the conclusions are summarized in Section VI.

II. SYSTEM MODEL

We consider a flying UAV and a sensing node, that can be placed at a rooftop in an urban/suburban environment, as shown in Fig. 1 and both the UAV and sensing node are equipped with omni-directional antenna.[1] The analysis is based on the assumption that the sensing node antenna is able to detect the UAV command, control and communication signals. We consider a passive cost-effective RF sensor for the 2.4 GHz and 5.8 GHz frequency bands where it can be deployed outdoors. Such RF sensor is equipped with omni-directional antenna for a wide frequency range, i.e. 20 MHz-18 GHz, and antenna gains are up to 5 dBi.

We assume that both the sensing node and the UAV are placed in the 3D cartesian coordinate system where the sensing node is located at $(x_d, y_d, z_d) \in \mathbb{R}^3$ with an elevation of z_d. On the other hand, the UAV can fly over higher altitudes, i.e. $z_u > z_d$ and the UAV is located at $(x_u, y_u, z_u) \in \mathbb{R}^3$.

In the presence of a target drone, the received signal $y \in \mathbb{C}$ at the sensing node is

$$y = \sqrt{P} h_i s + w, \quad i \in \{N, L\} \tag{1}$$

[1] Omni-directional antenna assumption in azimuthal direction is necessary as there is no prior knowledge of the intruding UAV location. This provides a 360-degrees coverage to detect the aerial target RF signal.

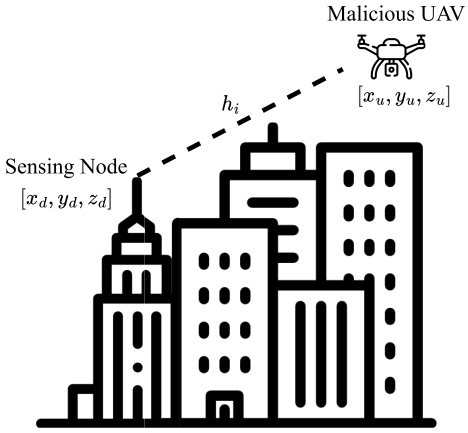

FIGURE 1. Received UAV signal at the sensing node.

where P is the UAV transmitted power, s is the unit-energy transmitted signal with zero mean and statistical expectation $\mathbb{E}[|s|^2] = 1$, h_i is the air-to-ground (A2G) fading channel gain where $i \in \{N, L\}$ denotes the NLoS or LoS channel conditions, respectively, and w is the complex additive white Gaussian noise (AWGN) with zero mean and variance $\sigma_0^2 = N_0/2$ for each of the in-phase and quadrature components.

A. AIR-TO-GROUND (A2G) CHANNEL

A2G channel between the UAV and the sensing node is subject to both LoS and NLoS conditions. The probability of a link having a LoS component at a given UAV coordinates is given by [39]

$$\mathrm{P_{LoS}} = \frac{1}{1 + a\exp\left\{-b\left[\frac{180}{\pi}\psi_u - a\right]\right\}} \tag{2}$$

where a and b are environment dependant constants, $\psi_u = \tan^{-1}((z_u - z_d)/r_u)$ is the UAV elevation AoA of the LoS link at the sensing node and $r_u = \sqrt{(x_u - x_d)^2 + (y_u - y_d)^2}$ is the horizontal distance from the UAV to the sensing node. The channel has NLoS components with a probability of $1 - \mathrm{P_{LoS}}$.

First, the multipath propagation under the NLoS condition follows the Rayleigh fading model, and channel gain is defined as [40]

$$h_N = \sqrt{\beta d^{-\rho}}\tilde{X} \tag{3}$$

where ρ is the corresponding path loss exponent of the link, β is the reference path loss at distance 1m, $d = \sqrt{r_u^2 + (z_u - z_d)^2}$ is the Euclidean distance between the UAV and the sensor, and $\tilde{X}$ represents the random scattering component modeled by a zero-mean and unit-variance circularly symmetric complex Gaussian (CSCG) random variable.

Furthermore, under the LoS conditions, the small-scale fading is modelled by Rician distribution, and channel gain is given by

$$h_L = \left(\sqrt{k\beta d^{-\rho}} + j\sqrt{k\beta d^{-\rho}}\right) + \sqrt{\beta d^{-\rho}}\tilde{X} \tag{4}$$

where k is the Rician factor. The SNR for both cases in the presence of a target is

$$\gamma_i = \frac{P\,|h_i|^2}{2\sigma_0^2}, \quad i \in \{N, L\}. \tag{5}$$

Unlike communication scenarios, where the aim at the receiver is to decode the signal, our interest here is to detect the presence of the UAV from its energy emitted. Hence, the decision criteria is based on the received signal strength (RSS) for a given UAV coordinates and channel conditions.

III. UAV DETECTION PROBLEM FORMULATION

The received signal[2] in (1) has both in-phase and quadrature components, i.e. $y = y_I + jy_Q$, and the RSS at the sensing node can be expressed as

$$R = y_I^2 + y_Q^2. \tag{6}$$

We consider binary hypothesis testing to detect the UAV presence based on the RSS at the sensing node. Here, the null hypothesis, $\mathcal{H}_0$, represents the state in which no drone is detected, and $y = w$ is a zero mean complex Gaussian random variable with variance $\mathbb{E}[yy^*] = \mathbb{E}[y_I^2] + \mathbb{E}[y_Q^2] = 2\sigma_0^2$, i.e. $y \sim \mathcal{N}_{\mathbb{C}}(0, 2\sigma_0^2)$. Under this hypothesis, the RSS is sum of the squares of two independent and identically distributed (i.i.d.) Gaussian random variables that follows exponential distribution, i.e. $R|\mathcal{H}_0 \sim \exp\{2\sigma_0^2\}$. For the alternative hypothesis, $\mathcal{H}_1$, representing the presence of the target drone, the distribution of the received signal is based on the LoS and NLoS conditions.

Considering the NLoS case, the received signal $y \sim \mathcal{N}_{\mathbb{C}}(0, 2\sigma_1^2)$ with $\sigma_1^2 = N_0/2 + P\beta d^{-\rho}$. Hence, the RSS under the alternative hypothesis follows exponential distribution, i.e. $R|\mathcal{H}_{1N} \sim \exp\{2\sigma_1^2\}$. As for the LoS case, the signal received under the alternative hypothesis is $y \sim \mathcal{N}_{\mathbb{C}}(\frac{\mu}{\sqrt{2}}, 2\sigma_1^2)$ and the RSS distribution is a non-central Chi-squared with two degrees of freedom, i.e. $R|\mathcal{H}_{1L} \sim \chi_2'^2(\mu)$, where $\mu = \sqrt{2kP\beta d^{-\rho}}$ is the non centrality parameter.

Furthermore, we represent the null and alternative hypotheses in terms of the conditional probability density function (PDF) of the RSS as

$$\mathcal{P}_{R|\mathcal{H}_0}(r|\mathcal{H}_0) = \frac{1}{2\sigma_0^2}e^{-\frac{r}{2\sigma_0^2}} \tag{7}$$

$$\mathcal{P}_{R|\mathcal{H}_{1i}}(r|\mathcal{H}_{1i}) = \begin{cases} \frac{1}{2\sigma_1^2}e^{-\frac{\mu^2+r}{2\sigma_1^2}} I_0\left(\frac{\mu}{\sigma_1^2}\sqrt{r}\right), & \text{for } i = L \\ \frac{1}{2\sigma_1^2}e^{-\frac{r}{2\sigma_1^2}}, & \text{for } i = N \end{cases} \tag{8}$$

where $I_0(.)$ denotes the zero-order modified Bessel function of the first kind.

[2]In the case of multiple antenna elements at the RF sensor, the mathematical analysis can be extended to a measurement vector of in-phase and quadrature components; however, it is beyond the scope of this work.

IV. UAV DETECTION PERFORMANCE

A. PROBABILITY OF DETECTION ANALYSIS

In this section, the probability of detection, $\mathbf{P}_D$, and the probability of false alarm, $\mathbf{P}_F$, are derived along with the probability of detection in terms of false alarm probability. Since the conditional PDF under $\mathcal{H}_0$ does not depend on the channel state, the expression of the probability of false alarm is given by

$$\mathbf{P}_F = \int_{\eta}^{\infty} \mathcal{P}_{R|\mathcal{H}_0}(r|\mathcal{H}_0)\, dr = \int_{\eta}^{\infty} \frac{e^{-\frac{r}{2\sigma_0^2}}}{2\sigma_0^2} dr = e^{-\frac{\eta}{2\sigma_0^2}} \tag{9}$$

where η is the decision threshold, which is derived in subsection IV-B. The decision threshold, therefore, can be expressed as a function of $\mathbf{P}_F$ as

$$\eta = -2\sigma_0^2 \ln \mathbf{P}_F \tag{10}$$

where $\ln(\cdot)$ denotes the natural logarithm. Furthermore, the probability of detection under NLoS conditions, following similar derivations in (9) and substituting σ_0^2 and σ_1^2 yields

$$\mathbf{P}_{DN} = \exp\left(\ln \mathbf{P}_F / \left(1 + \frac{2P\beta}{N_0 d^{\rho}}\right)\right). \tag{11}$$

The expression of the probability of detection under LoS scenarios, according to [41], is defined as

$$\begin{aligned}\mathbf{P}_{DL} &= \int_{\frac{\sqrt{\eta}}{\sigma_1}}^{\infty} r e^{-\frac{(\frac{\mu}{\sigma_1})^2 + r^2}{2}} I_0\left(\frac{\mu}{\sigma_1} r\right) dr \\ &= Q_1\left(\frac{\mu}{\sigma_1}, \frac{\sqrt{\eta}}{\sigma_1}\right)\end{aligned} \tag{12}$$

where $Q_1(.,.)$ denotes the first order Marcum Q-function. After substituting the threshold in (10), μ, and σ_1 in (12), we have

$$\mathbf{P}_{DL} = Q_1\left(\sqrt{\frac{4kP\beta}{2P\beta + N_0 d^{\rho}}}, \sqrt{\frac{-\ln \mathbf{P}_F}{0.5 + \frac{P\beta}{N_0 d^{\rho}}}}\right). \tag{13}$$

Note that for a fixed $\mathbf{P}_F$, the probability of detection in (11) and (13) will degrade as noise variance, distance or path loss exponent increases. However, for larger UAV transmission power or Rician k factor, the detection performance will improve. Considering both LoS and NLoS, and environmental conditions at the sensing node, the average probability of detection for a fixed probability of false alarm, given UAV coordinates,[3] can be expressed as

$$\begin{aligned}\mathbf{P}_D = {} & \mathrm{P}_{\mathrm{LoS}}\, Q_1\left(\sqrt{\frac{4kP\beta}{2P\beta + N_0 d^{\rho}}}, \sqrt{\frac{-\ln \mathbf{P}_F}{0.5 + \frac{P\beta}{N_0 d^{\rho}}}}\right) \\ & + (1 - \mathrm{P}_{\mathrm{LoS}})\ \exp\left(\ln \mathbf{P}_F / \left(1 + \frac{2P\beta}{N_0 d^{\rho}}\right)\right).\end{aligned} \tag{14}$$

[3]Similar to the earlier works in [5] and [11], we assume an acquisition of the UAV coordinates and channel exist for the probability of detection derivations.

B. OPTIMUM DETECTOR

In this section, we utilize a statistical LLR test to optimize the choice of the decision threshold at the sensing node. The LLR expression under the NLoS channel condition is expressed as

$$\ln(\Lambda|_{\mathrm{N}}\mathcal{R}) \triangleq \ln\left(\frac{\mathcal{P}_{R|\mathcal{H}_{1N}}(r|\mathcal{H}_{1N})}{\mathcal{P}_{R|\mathcal{H}_0}(r|\mathcal{H}_0)}\right) \gtrless \ln \zeta \tag{15}$$

where $\ln(\Lambda|_{\mathrm{N}}\mathcal{R})$ represents the LLR under NLoS state and ζ depends on the a priori probabilities and the error cost under each hypothesis [42]. In our analysis, we assume equal a priori probabilities; hence, $\zeta = 1$ and $\ln \zeta = 0$. The detection decision depends on the received and observed values of r, representing the sufficient statistics to make the optimal decision. By solving (15) for r under equal probable hypotheses, we obtain

$$\begin{aligned}&\ln\left(\frac{\sigma_0^2}{\sigma_1^2}\right) - r\left[\frac{1}{2\sigma_1^2} - \frac{1}{2\sigma_0^2}\right] \gtrless 0 \\ &r \gtrless \frac{2\sigma_1^2\sigma_0^2}{\sigma_0^2 - \sigma_1^2} \ln\left(\frac{\sigma_0^2}{\sigma_1^2}\right).\end{aligned} \tag{16}$$

Substituting σ_0^2 and σ_1^2 in (16) to evaluate the NLoS optimum threshold η_N results in

$$\eta_N = \left(\frac{N_0^2 d^{\rho}}{2P\beta} + N_0\right) \ln\left(1 + \frac{2P\beta}{N_0 d^{\rho}}\right). \tag{17}$$

Following the same approach for calculating the optimum threshold under LoS, we represent the LLR as

$$\ln(\Lambda|_{\mathrm{L}}\mathcal{R}) \triangleq \ln\left(\frac{\mathcal{P}_{R|\mathcal{H}_{1L}}(r|\mathcal{H}_{1L})}{\mathcal{P}_{R|\mathcal{H}_0}(r|\mathcal{H}_0)}\right) \gtrless \ln \zeta, \tag{18}$$

and after solving for the sufficient statistic r considering equal probable hypotheses, this leads to

$$\begin{aligned}&\ln\left(\frac{\sigma_0^2\, e^{-\frac{\mu^2 + r}{2\sigma_1^2}} I_0\left(\frac{\mu\sqrt{r}}{\sigma_1^2}\right)}{\sigma_1^2\, e^{-\frac{r}{2\sigma_0^2}}}\right) \gtrless 0 \\ &r - \frac{2\sigma_1^2\sigma_0^2}{\sigma_0^2 - \sigma_1^2} \ln\left(I_0\left(\frac{\mu\sqrt{r}}{\sigma_1^2}\right)\right) \gtrless \frac{2\sigma_1^2\sigma_0^2}{\sigma_0^2 - \sigma_1^2} \\ &\left(\ln\left(\frac{\sigma_0^2}{\sigma_1^2}\right) - \frac{\mu^2}{2\sigma_1^2}\right)\end{aligned} \tag{19}$$

where $\ln(\Lambda|_{\mathrm{L}}\mathcal{R})$ is the derived LLR assuming LoS conditions. The cumbersome expression in (19) can not be simplified in terms of the sufficient statistic r, which leads to high complexity in the design of an optimum detector. We propose in the following subsection a simplified low-complexity detector to overcome this point with reasonable performance.

C. PROPOSED LOW-COMPLEXITY DETECTOR

Due to the sensitivity of the threshold-based detection technique, a slight change in such threshold can considerably increase the error probability, i.e. the probabilities of false

alarm and miss detection. Therefore, it is crucial for the sensing node to decide on an appropriate threshold. We first define Ψ to be the weighted average of the RSS, R, under both hypotheses which is given by

$$\begin{aligned}\Psi &= \epsilon\, \mathbb{E}[R|\mathcal{H}_1] + (1-\epsilon)\, \mathbb{E}[R|\mathcal{H}_0] \\ &= 2\epsilon\sigma_1^2 + \epsilon\mu^2 + 2\sigma_0^2 - 2\epsilon\sigma_0^2 \end{aligned} \tag{20}$$

where ϵ is the weighting factor that represent the contribution of $\mathcal{H}_1$ on Ψ such that $0 < \epsilon < 1$. Therefore, the expression of the suboptimal threshold under the LoS channel state, η_L, can be expressed using (20) as

$$\begin{aligned}\eta_L = &-\left(\frac{N_0^2 d^\rho}{2P\beta} + N_0\right) \\ &\times\left(\ln\left(\frac{1}{1+\frac{2P\beta}{N_0 d^\rho}} I_0\left(\frac{\sqrt{2kP\beta d^{-\rho}\Psi}}{\frac{N_0}{2}+P\beta d^{-\rho}}\right)\right) - \frac{k}{1+\frac{N_0 d^\rho}{2P\beta}}\right).\end{aligned} \tag{21}$$

It can be seen that increasing Ψ results in smoothing the decision threshold with higher detection probabilities at the cost of increasing the false alarm probability. Thus, the selection of ϵ depends on the channel state at the sensing node where higher values are usually chosen at low SNRs. To tackle this problem, we introduce the average overall error probability at the sensing node, ϕ, as

$$\phi = \frac{1 - \mathbf{P}_{DL} + \mathbf{P}_F}{2}, \tag{22}$$

which is the average of the miss detection probability and the probability of false alarm. Hence, we can formulate the objective function to optimize the parameter ϵ as

$$\hat{\epsilon} = \underset{0\le\epsilon\le1}{\arg\min} \quad \phi(\Psi) \tag{23}$$

where $\hat{\epsilon}$ is the optimized ϵ value. To solve the problem in (23), we propose an iterative algorithm to obtain ϵ that minimizes the average overall error probability, ϕ, as shown in Algorithm 1. In this algorithm, we start by defining a vector, $\boldsymbol{\epsilon}$, of different values of $\boldsymbol{\epsilon}(i) \in [0, 1]$ with intervals of $\frac{1}{\kappa}$, and an initial value of $\hat{\epsilon} = 0$ at the first iteration with an assumption of a maximum average error (average error probability $\hat{\phi} = 0.5$). From here, we use the equations (20), (21), and (22) to evaluate the value of the average error at the $\hat{\epsilon} = 0$. Using the condition of the average error being less than the previously defined value, we keep updating the value of $\hat{\epsilon}$ by adding $\frac{1}{\kappa}$. We note that the algorithm will stop its iteration when the value of the average error at ith iteration is less than the error of $(i+1)$th iteration, which is assured due to the convexity of average error function. Moreover, it is worth mentioning that the convergence speed and accuracy of this algorithm depends on the selection of κ, where higher values will improve the accuracy at the cost of the number of iterations required to reach the optimal value of ϵ.

It is important to notice that the intruding UAV is expected to be in the far field region with respect to the sensing node. Hence, the impact of the minor changes in average SNR and/or the UAV location will have no significant impact in the selection of the optimum value of ϵ. However, for a near-field scenarios, we expect the proposed algorithm will be updating the optimum value of ϵ more rapidly, which can be an extension of the current work.

Algorithm 1 Proposed Algorithm to Solve (23)

1: define a vector $\boldsymbol{\epsilon} = [0, \frac{1}{\kappa}, \frac{2}{\kappa}, \ldots, 1]$ with a proper κ value
2: define $\hat{\phi} = 0.5$, $\hat{\epsilon} = 0$ and $i = 1$ as initial values
3: evaluate Ψ at $\boldsymbol{\epsilon}(i)$ from (20)
4: evaluate η_L and ϕ from (21) and (22)
5: **while** $\phi < \hat{\phi}$ **do**
6: $\quad\hat{\phi} \leftarrow \phi$
7: $\quad\hat{\epsilon} \leftarrow \boldsymbol{\epsilon}(i)$
8: $\quad i \leftarrow i + 1$
9: $\quad$update Ψ at $\boldsymbol{\epsilon}(i)$
10: $\quad$update η_L and ϕ
11: **end while**
12: **return** $\hat{\epsilon}$

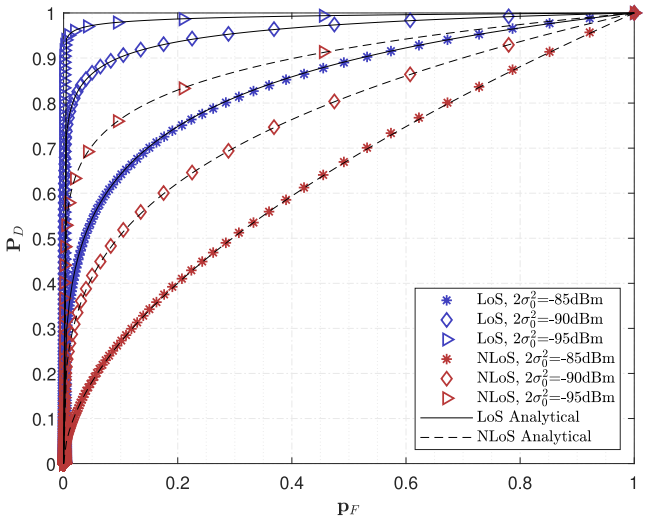

FIGURE 2. ROCs for LoS/NLoS scenarios and various noise variance $2\sigma_0^2$. The black solid lines represent the analytical results under LoS, while the dashed lines for NLoS.

Further, under the assumption that the LoS/NLoS channel state is well estimated at the sensing node, the average probability of detection in low-complexity suboptimal receiver using the derived thresholds is

$$\begin{aligned}\mathbf{P}_D = \mathrm{P}_{\mathrm{LoS}} \times Q_1\left(\sqrt{\frac{2k}{1+\frac{N_0 d^\rho}{2P\beta}}}, \sqrt{\frac{\eta_L}{N_0/2 + P\beta d^{-\rho}}}\right) \\ + (1 - \mathrm{P}_{\mathrm{LoS}}) \times e^{-\frac{\eta_N}{N_0 + 2P\beta d^{-\rho}}}.\end{aligned} \tag{24}$$

However, if no prior information at the sensing node about the conditions whether LoS or NLoS, then an average threshold, η_{avg}, can be used such that $\eta_{\mathrm{avg}} = 0.5\eta_L + 0.5\eta_N$.

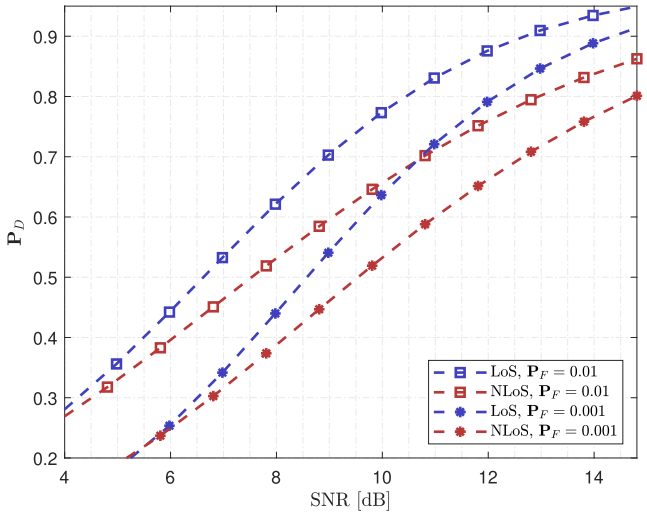

FIGURE 3. Probability of UAV detection with $\mathbf{P}_F = 0.01$ and 0.001 under LoS/NLoS conditions.

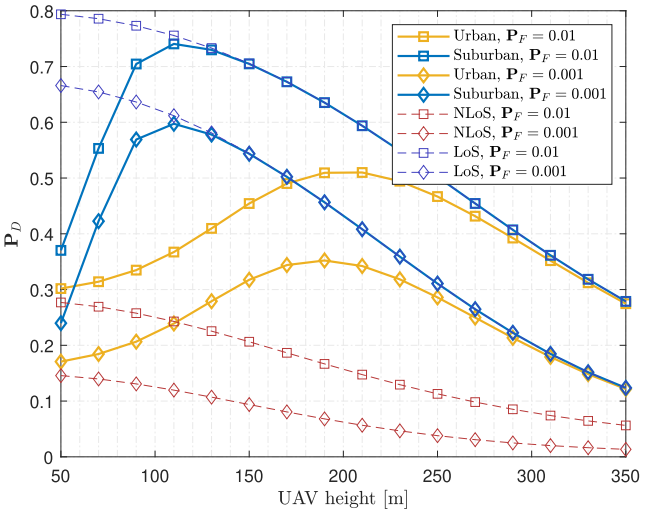

FIGURE 4. Probability of UAV detection as a function of its altitude in urban and suburban environments.

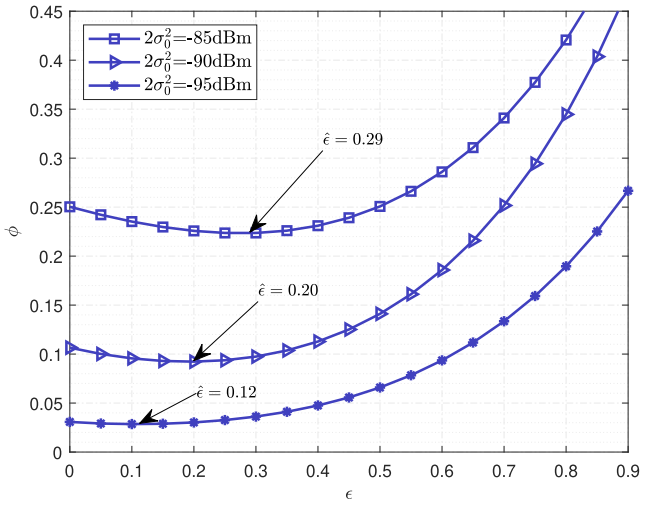

FIGURE 5. Average overall error probability and optimized parameter $\hat{\epsilon}$ in proposed detector.

V. NUMERICAL RESULTS

For our numerical analysis, we set the parameters as in Table 3 where the values of a and b are chosen according to [39], which is based on the International Telecommunication Union (ITU) model. This model considers the density ratio of built-up land area to the total land area, mean number of buildings per unit area, and the buildings' height distribution. It is critical, indeed, in such performance analysis investigations to select proper and realistic system parameters, where the system behavior is sensitive to such parameters. For this reason, we have meticulously selected them to be within the realistic and acceptable range. For example, the choice of the UAV emitted power, $P = 27$dBm, is in line with the values reported in literature ranging from 24-27dBm, [11], [43]. Moreover, the path loss exponent, ρ, has a noticeable effect on the overall system performance. We assume $\rho = 3.5$ which is a practical value and represents the urban and suburban environments where a range of 2-5 have been discussed in [44] for various wireless environments. The UAV and sensing node locations have been chosen randomly to fairly test the performance of the system.

In Fig. 2, we present the receiver operating characteristic (ROC), where detection performance is depicted as a function of $\mathbf{P}_F$ at the sensing node. This is obtained using (11) and (13) under both NLoS and LoS scenarios, respectively, with $2\sigma_0^2 \in \{-95, -90, -85\}$ in dBm. The numerical simulations are carried out by generating random samples of the conditional probability density functions of the received signal strength under both LoS and NLoS, and then we use a moving threshold to evaluate the probability of detection and the probability of false alarm at every instant to calculate the ROCs. Moreover, 5×10^4 Monte Carlo simulation trials have been performed to validate the derived mathematical expressions. The ROC curves through numerical simulation, shown in Fig. 2, match well the derived expressions. ROC curves show that even for a lower variance of noise under NLoS cases, the LoS channel condition will result in better performance due to the existence of the direct path component. Nevertheless, this could change based on the choice of the Rician factor k that may alter the performance under the LoS scenarios.

In Fig. 3, the performance of the UAV detection is illustrated under various SNR values for both LoS and NLoS environments. It is noticed that even under the same SNR and fixed $\mathbf{P}_F$, there is higher probability of detection when a direct LoS link exists. This is due to the existence of the non-zero mean and the skewed shape of the non-central Chi-squared distribution. In such case, the area under the alternative hypothesis conditional PDF will be larger than the NLoS case where it is exponentially distributed for both $\mathcal{H}_0$ and $\mathcal{H}_{1N}$.

On the other hand, Fig. 4 demonstrates the effect of the UAV height on $\mathbf{P}_D$ using (14) for both urban and suburban environments compared to the conditionally known LoS

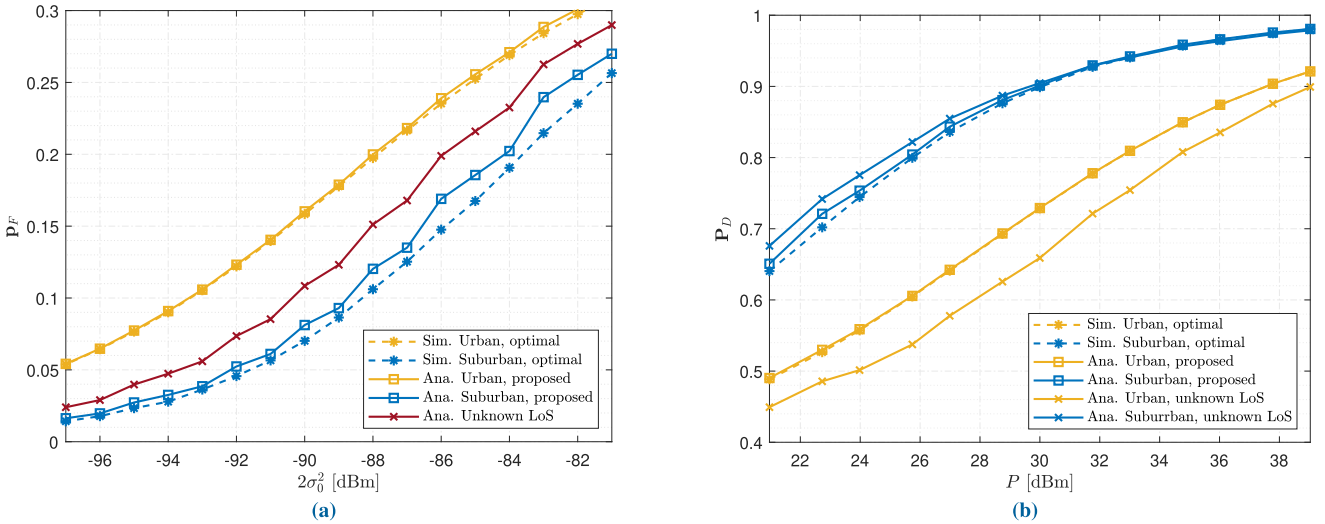

FIGURE 6. Performance evaluation of the proposed suboptimal low-complexity detector.

or NLoS cases. Due to averaging, it is shown that the conditionally known LoS and NLoS are in fact the upper and lower bounds for the probability of detection, where both environmental expressions will almost match the NLoS state at very low altitudes and will perfectly match the LoS at high altitudes. Note that although the distance between the UAV and the sensing node increases with the UAV height, the probability of detection will continue to increase until reaching its maximum $\mathbf{P}_D$ of about 0.75 at around $z_u = 120$m (suburban) and about 0.5 at around $z_u = 190$m (urban). This is due to the fact that UAVs at relatively higher altitudes, to some extent, will have larger $\mathrm{P_{LoS}}$. Such improved LoS conditions will enhance the detection probability, $\mathbf{P}_D$, even though the degradation due to free-space path loss increases with increased range between the UAV and sensing node. On the other hand, once $\mathrm{P_{LoS}} \approx 1$, then $\mathbf{P}_D$ decreases as the UAV is flying away from the sensing node. There is around 0.15 increase in $\mathbf{P}_D$ when $\mathbf{P}_F$ rises from 0.001 to 0.01 at LoS conditions, where $\mathbf{P}_D \approx 0.8$ at low UAV altitudes. In NLoS cases, however, a quite weaker performance and lower gains are achieved when rising $\mathbf{P}_F$.

Fig. 5 illustrates the average overall error probability for different choices of ϵ with $2\sigma_0^2 \in \{-95, -90, -85\}$ in dBm, i.e. different SNRs. It is noted that the convexity of the average overall error function ϕ, i.e. it is convex with a global minimum value. Hence, our proposed algorithm will keep updating the value of $\hat{\epsilon}$ in an iterative manner, until it reaches an index where the error of the previous iteration was lower. At this stage, the algorithm will break the loop to avoid unnecessary calculations. Besides, the optimum value for ϵ will decrease with lower noise and higher SNRs, leading to stricter decision criteria and lower false alarm probabilities.

Fig. 6 illustrates the detection performance for the proposed suboptimal low-complexity detector at $\kappa = 25$ and under different environmental scenarios while increasing the noise variance, $2\sigma_0^2$, and the UAV transmitted power, P, in Figs. 6a and 6b, respectively.

TABLE 3. System and environment parameters for monte-carlo simulations.

Parameter	Value	Parameter	Value
P	27 dBm	ρ	3.5
k	5 dB	N_0	-90 dBm
β	-30 dB	d	290.2 m
(x_d, y_d, z_d)	$(0, 0, 25)$	(x_u, y_u, z_u)	$(200, 200, 90)$
Urban (a,b)	(9.6117, 0.1581)	Suburban (a,b)	(4.88, 0.429)

In Fig. 6a, we evaluate $\mathbf{P}_F$ numerically under the optimum threshold of LoS using (19) and compare it to our proposed suboptimal threshold in (21). The results show that the proposed suboptimal threshold has comparable performance to the optimal curves. Furthermore, since $\hat{\epsilon}$ is optimized for the considered noise variance, it is notable that the slope of the suboptimal threshold, $\hat{\epsilon}$, is updated, every 2-4 dBm to maintain lower error probability and get closer to the optimal one. Besides, as we increase κ, the slope of the suboptimal curves will be smoother and will eventually get closer the optimal threshold as the algorithm will run more iterations and will reach to an accurate selection of $\hat{\epsilon}$. In urban areas, the probability of LoS existence is small compared to suburban environment, i.e. $\mathrm{P_{LoS}}$ is 0.15 and 0.86 for urban and suburban environments, respectively, which affects the LoS component contribution. Furthermore, if the LoS/NLoS status is unknown, $\mathbf{P}_F$ will be the same irrespective of the environment condition because we use η_{avg} where both LoS/NLoS have the same RSS distribution under $\mathcal{H}_0$.

In Fig. 6b, the average probability of detection is shown with varying UAV transmit power. It can be seen that the probability of detection under our proposed threshold has a higher detection probability at some instants than the optimum one. However, the overall accuracy of the

TABLE 4. Confusion matrices for LoS thresholds.

(a) Optimal

Actual \ Pred.	$\mathcal{H}_0$	$\mathcal{H}_1$
$\mathcal{H}_0$	47,311	2,689
$\mathcal{H}_1$	6,504	43,496

(b) Suboptimal

Actual \ Pred.	$\mathcal{H}_0$	$\mathcal{H}_1$
$\mathcal{H}_0$	46,612	3,388
$\mathcal{H}_1$	6,029	43,917

optimum threshold is better, which is compensated by the probability of false alarm. It is also worth mentioning that the performance under unknown LoS condition will vary across the different environments as the mathematical expression for $\mathbf{P}_D$ depends on LoS and NLoS conditions. It can be seen that due to averaging, the smoothed threshold under suburban environment will have higher $\mathbf{P}_D$, while the restricted threshold in urban environments will have a much lower $\mathbf{P}_D$.

Finally, Table 4 presents the confusion matrices of the optimal criteria under LoS channel and the proposed one at $\kappa = 25$, which are computed using 5×10^4 Monte Carlo simulation trials. Although the proposed threshold has slightly lower probability of miss detection, $\mathrm{P}_{\mathcal{H}_0|\mathcal{H}_1}$, than the optimal threshold, the probability of false alarm, $\mathrm{P}_{\mathcal{H}_1|\mathcal{H}_0}$, is higher in the suboptimal case. However, the overall accuracy rate is 0.905 for the suboptimal threshold, which is close to the optimal case having an accuracy of 0.908. It is important to note that the performance of the proposed threshold is highly dependant on the choice of the value of κ, where the accuracy will get closer to the optimal threshold as κ increases. However, this comes at the cost of computational complexity.

VI. CONCLUSION

In this paper, we investigated an RSS-based passive detection approach under a realistic Rician fading channel model and considered the air-to-ground channel conditions. Furthermore, we demonstrated the use of the optimum threshold criteria at the sensing node under NLoS state and proposed a low-complexity sub-optimum threshold under LoS channel conditions based on the LLR. Our performance analysis and closed-form derived analytical expressions have been verified using extensive Monte Carlo simulations. The analytical and simulation results showed that an overall accuracy rate of above 0.9 is achieved under LoS cases and a high probability of detection for a fixed false alarm probability can be attained as well. However, the detection accuracy at sensing node under NLoS conditions is lower but can be improved with the deployment of multiple sensing nodes. Moreover, the detection performance at the sensing node, and our obtained results can be coupled with proper deep learning techniques in future work to tackle more challenging scenarios. For instance, deep learning can be used to find the optimal placement of multiple low-cost sensing nodes given the 3D visualization of outdoor scene, or to simultaneously combine multiple detection mechanisms to detect a swarm of UAVs.

REFERENCES

[1] H. El-Sayed, M. Chaqfa, S. Zeadally, and D. Puthal, "A traffic-aware approach for enabling unmanned aerial vehicles (UAVs) in smart city scenarios," *IEEE Access*, vol. 7, pp. 86297–86305, 2019.

[2] F. Mohammed, A. Idries, N. Mohamed, J. Al-Jaroodi, and I. Jawhar, "UAVs for smart cities: Opportunities and challenges," in *Proc. Int. Conf. Unmanned Aircr. Syst. (ICUAS)*, 2014, pp. 267–273.

[3] I. Guvenc, F. Koohifar, S. Singh, M. L. Sichitiu, and D. Matolak, "Detection, tracking, and interdiction for amateur drones," *IEEE Commun. Mag.*, vol. 56, no. 4, pp. 75–81, Apr. 2018.

[4] G. Ji, C. Song, and H. Huo, "Detection and identification of low-slow-small rotor unmanned aerial vehicle using micro-Doppler information," *IEEE Access*, vol. 9, pp. 99995–100008, 2021.

[5] P. Sinha, I. Güvenç, and M. C. Gürsoy, "Fundamental limits on detection of UAVs by existing terrestrial RF networks," *IEEE Open J. Commun. Soc.*, vol. 2, pp. 2111–2130, 2021.

[6] X. Shi, C. Yang, W. Xie, C. Liang, Z. Shi, and J. Chen, "Anti-drone system with multiple surveillance technologies: Architecture, implementation, and challenges," *IEEE Commun. Mag.*, vol. 56, no. 4, pp. 68–74, Apr. 2018.

[7] S. Park, S. Lee, and N. Kwak, "Range-Doppler map augmentation by generative adversarial network for deep UAV classification," in *Proc. IEEE Radar Conf.*, Mar. 2022, pp. 1–7.

[8] M. L. Pawelczyk and M. Wojtyra, "Real world object detection dataset for quadcopter unmanned aerial vehicle detection," *IEEE Access*, vol. 8, pp. 174394–174409, 2020.

[9] J. Zhao, J. Zhang, D. Li, and D. Wang, "Vision-based anti-UAV detection and tracking," *IEEE Trans. Intell. Transp. Syst.*, vol. 23, no. 12, pp. 25323–25334, Dec. 2022.

[10] N. Soltani, G. Reus-Muns, B. Salehi, J. Dy, S. Ioannidis, and K. Chowdhury, "RF fingerprinting unmanned aerial vehicles with non-standard transmitter waveforms," *IEEE Trans. Veh. Technol.*, vol. 69, no. 12, pp. 15518–15531, Dec. 2020.

[11] S. Al-Dharrab, "Detection performance of malicious UAV using massive IoT networks," in *Proc. IEEE 97th Veh. Technol. Conf. (VTC-Spring)*, Jun. 2023, pp. 1–5.

[12] M. Z. Anwar, Z. Kaleem, and A. Jamalipour, "Machine learning inspired sound-based amateur drone detection for public safety applications," *IEEE Trans. Veh. Technol.*, vol. 68, no. 3, pp. 2526–2534, Mar. 2019.

[13] H. Du, D. Niyato, Y.-A. Xie, Y. Cheng, J. Kang, and D. I. Kim, "Performance analysis and optimization for jammer-aided multiantenna UAV covert communication," *IEEE J. Sel. Areas Commun.*, vol. 40, no. 10, pp. 2962–2979, Oct. 2022.

[14] W. Nie, Z.-C. Han, M. Zhou, L.-B. Xie, and Q. Jiang, "UAV detection and identification based on WiFi signal and RF fingerprint," *IEEE Sensors J.*, vol. 21, no. 12, pp. 13540–13550, Jun. 2021.

[15] M. Ezuma, F. Erden, C. Kumar Anjinappa, O. Ozdemir, and I. Guvenc, "Detection and classification of UAVs using RF fingerprints in the presence of Wi-Fi and Bluetooth interference," *IEEE Open J. Commun. Soc.*, vol. 1, pp. 60–76, 2020.

[16] F.-L. Chiper, A. Martian, C. Vladeanu, I. Marghescu, R. Craciunescu, and O. Fratu, "Drone detection and defense systems: Survey and a software-defined radio-based solution," *Sensors*, vol. 22, no. 4, p. 1453, Feb. 2022.

[17] M. Ezuma, F. Erden, C. K. Anjinappa, O. Ozdemir, and I. Guvenc, "Micro-UAV detection and classification from RF fingerprints using machine learning techniques," in *Proc. IEEE Aerosp. Conf.*, Mar. 2019, pp. 1–13.

[18] Y. Mo, J. Huang, and G. Qian, "Deep learning approach to UAV detection and classification by using compressively sensed RF signal," *Sensors*, vol. 22, no. 8, p. 3072, Apr. 2022.

[19] I. Nemer, T. Sheltami, I. Ahmad, A. U.-H. Yasar, and M. A. R. Abdeen, "RF-based UAV detection and identification using hierarchical learning approach," *Sensors*, vol. 21, no. 6, p. 1947, Mar. 2021.

[20] D.-I. Noh, S.-G. Jeong, H.-T. Hoang, Q.-V. Pham, T. Huynh-The, M. Hasegawa, H. Sekiya, S.-Y. Kwon, S.-H. Chung, and W.-J. Hwang, "Signal preprocessing technique with noise-tolerant for RF-based UAV signal classification," *IEEE Access*, vol. 10, pp. 134785–134798, 2022.

[21] M. Zuo, S. Xie, X. Zhang, and M. Yang, "Recognition of UAV video signal using RF fingerprints in the presence of WiFi interference," *IEEE Access*, vol. 9, pp. 88844–88851, 2021.

[22] J. Hu, Y. Wu, R. Chen, F. Shu, and J. Wang, "Optimal detection of UAV's transmission with beam sweeping in covert wireless networks," *IEEE Trans. Veh. Technol.*, vol. 69, no. 1, pp. 1080–1085, Jan. 2020.

[23] N. V. Abhishek, M. N. Aman, T. J. Lim, and B. Sikdar, "MaDe: Malicious aerial vehicle detection using generalized likelihood ratio test," in *Proc. IEEE Int. Conf. Commun.*, Feb. 2022, pp. 1–6.
[24] C. Wang, J. Tian, J. Cao, and X. Wang, "Deep learning-based UAV detection in pulse-Doppler radar," *IEEE Trans. Geosci. Remote Sens.*, vol. 60, 2022, Art. no. 5105612.
[25] Y. Yang, F. Yang, L. Sun, T. Xiang, and P. Lv, "Echoformer: Transformer architecture based on radar echo characteristics for UAV detection," *IEEE Sensors J.*, vol. 23, no. 8, pp. 8639–8653, Apr. 2023.
[26] Y. Li, M. Fu, H. Sun, Z. Deng, and Y. Zhang, "Radar-based UAV swarm surveillance based on a two-stage wave path difference estimation method," *IEEE Sensors J.*, vol. 22, no. 5, pp. 4268–4280, Mar. 2022.
[27] M. Ezuma, O. Ozdemir, C. K. Anjinappa, W. A. Gulzar, and I. Guvenc, "Micro-UAV detection with a low-grazing angle millimeter wave radar," in *Proc. IEEE Radio Wireless Symp. (RWS)*, Jan. 2019, pp. 1–4.
[28] M. Ezuma, C. K. Anjinappa, M. Funderburk, and I. Guvenc, "Radar cross section based statistical recognition of UAVs at microwave frequencies," *IEEE Trans. Aerosp. Electron. Syst.*, vol. 58, no. 1, pp. 27–46, Feb. 2022.
[29] J. Klare, O. Biallawons, and D. Cerutti-Maori, "UAV detection with MIMO radar," in *Proc. 18th Int. Radar Symp. (IRS)*, 2017, pp. 1–8.
[30] S. N. Aspragkathos, G. C. Karras, and K. J. Kyriakopoulos, "A hybrid model and data-driven vision-based framework for the detection, tracking and surveillance of dynamic coastlines using a multirotor UAV," *Drones*, vol. 6, no. 6, p. 146, Jun. 2022.
[31] K. Lu, R. Xu, J. Li, Y. Lv, H. Lin, and Y. Liu, "A vision-based detection and spatial localization scheme for forest fire inspection from UAV," *Forests*, vol. 13, no. 3, p. 383, Feb. 2022.
[32] B. Wei and M. Barczyk, "Experimental evaluation of computer vision and machine learning-based UAV detection and ranging," *Drones*, vol. 5, no. 2, p. 37, May 2021.
[33] R. Opromolla, G. Fasano, and D. Accardo, "A vision-based approach to UAV detection and tracking in cooperative applications," *Sensors*, vol. 18, no. 10, p. 3391, Oct. 2018.
[34] P. Casabianca and Y. Zhang, "Acoustic-based UAV detection using late fusion of deep neural networks," *Drones*, vol. 5, no. 3, p. 54, Jun. 2021.
[35] I. Aydin and E. Kizilay, "Development of a new light-weight convolutional neural network for acoustic-based amateur drone detection," *Appl. Acoust.*, vol. 193, May 2022, Art. no. 108773.
[36] W. Wang, K. Fan, Q. Ouyang, and Y. Yuan, "Acoustic UAV detection method based on blind source separation framework," *Appl. Acoust.*, vol. 200, Nov. 2022, Art. no. 109057.
[37] Z. Shi, X. Chang, C. Yang, Z. Wu, and J. Wu, "An acoustic-based surveillance system for amateur drones detection and localization," *IEEE Trans. Veh. Technol.*, vol. 69, no. 3, pp. 2731–2739, Mar. 2020.
[38] H. Liu, K. Fan, Q. Ouyang, and N. Li, "Real-time small drones detection based on pruned YOLOv4," *Sensors*, vol. 21, no. 10, p. 3374, May 2021.
[39] A. Al-Hourani, S. Kandeepan, and S. Lardner, "Optimal LAP altitude for maximum coverage," *IEEE Wireless Commun. Lett.*, vol. 3, no. 6, pp. 569–572, Dec. 2014.
[40] S. Li, B. Duo, X. Yuan, Y.-C. Liang, and M. Di Renzo, "Reconfigurable intelligent surface assisted UAV communication: Joint trajectory design and passive beamforming," *IEEE Wireless Commun. Lett.*, vol. 9, no. 5, pp. 716–720, May 2020.
[41] J. G. Proakis and M. Salehi, *Digital Communications*, 5th ed. New York, NY, USA: McGraw-Hill, 2008.
[42] H. L. Van Trees, *Detection, Estimation, and Modulation Theory, Part I: Detection, Estimation, and Linear Modulation Theory*. Hoboken, NJ, USA: Wiley, 2004.
[43] P. Mursia, F. Devoti, V. Sciancalepore, and X. Costa-Pérez, "RISe of flight: RIS-empowered UAV communications for robust and reliable air-to-ground networks," *IEEE Open J. Commun. Soc.*, vol. 2, pp. 1616–1629, 2021.
[44] T. Rappaport, *Wireless Communications: Principles and Practice*, 2nd ed. Upper Saddle River, NJ, USA: Prentice-Hall, 2001.

YOUSEF AWAD (Student Member, IEEE) received the B.Sc. degree in communication and networks engineering from Prince Sultan University, Riyadh, Saudi Arabia, in 2020, and the M.Sc. degree in telecommunication engineering from the King Fahd University of Petroleum and Minerals (KFUPM), Dhahran, Saudi Arabia, in 2024. He is currently pursuing the Ph.D. degree with the Department of Electrical and Computer Engineering, King Abdullah University of Science and Technology (KAUST), Thuwal, Saudi Arabia. During the M.Sc. studies, he was a Telecommunication Engineer with King Fahd International Airport (KFIA), Dammam, Saudi Arabia, with Enova by Veolia. His research interests include wireless communication systems, unmanned aerial vehicles (UAVs) detection, and reconfigurable intelligent surfaces (RISs) applications.

SUHAIL AL-DHARRAB (Senior Member, IEEE) received the B.Sc. degree in electrical engineering from the King Fahd University of Petroleum and Minerals, Dhahran, Saudi Arabia, in 2005, and the M.A.Sc. and Ph.D. degrees in electrical and computer engineering from the University of Waterloo, Waterloo, ON, Canada, in 2009 and 2013, respectively. From 2005 to 2007, he was a Graduate Assistant with the Electrical Engineering Department, King Fahd University of Petroleum and Minerals. In 2015, he was a Visiting Professor with the School of Electrical and Computer Engineering, Georgia Institute of Technology, Atlanta, GA, USA. He is currently an Assistant Professor with the Electrical Engineering Department, an Affiliate Member with the Interdisciplinary Research Center for Communication Systems and Sensing, and the Assistant Dean of Research with the King Fahd University of Petroleum and Minerals. His research interests include wireless communication systems, underwater acoustic communication, digital signal processing, and information theory.